

2015

Chemical-free inactivated whole influenza virus vaccine prepared by ultrashort pulsed laser treatment

Shaw-Wei David Tsen

Washington University School of Medicine in St. Louis

Nisha Donthi

Johns Hopkins Medical Institutions

Victor La

Johns Hopkins Medical Institutions

Wen-Han Hsieh

Johns Hopkins Medical Institutions

Yen-Der Li

National Taiwan University

See next page for additional authors

Follow this and additional works at: https://digitalcommons.wustl.edu/open_access_pubs

Recommended Citation

Tsen, Shaw-Wei David; Donthi, Nisha; La, Victor; Hsieh, Wen-Han; Li, Yen-Der; Knoff, Jayne; Chen, Alexander; Wu, Tzyy-Choou; Hung, Chien-Fu; Achilefu, Samuel; and Tsen, Kong-Thon, "Chemical-free inactivated whole influenza virus vaccine prepared by ultrashort pulsed laser treatment." *Journal of Biomedical Optics*.20,5. 051008. (2015).
https://digitalcommons.wustl.edu/open_access_pubs/7502

Authors

Shaw-Wei David Tsen, Nisha Donthi, Victor La, Wen-Han Hsieh, Yen-Der Li, Jayne Knoff, Alexander Chen, Tzyy-Chouu Wu, Chien-Fu Hung, Samuel Achilefu, and Kong-Thon Tsen

Chemical-free inactivated whole influenza virus vaccine prepared by ultrashort pulsed laser treatment

Shaw-Wei David Tsen
Nisha Donthi
Victor La
Wen-Han Hsieh
Yen-Der Li
Jayne Knoff
Alexander Chen
Tzyy-Choou Wu
Chien-Fu Hung
Samuel Achilefu
Kong-Thon Tsen

Chemical-free inactivated whole influenza virus vaccine prepared by ultrashort pulsed laser treatment

Shaw-Wei David Tsen,^a Nisha Donthi,^b Victor La,^b Wen-Han Hsieh,^b Yen-Der Li,^c Jayne Knoff,^b Alexander Chen,^b Tzyy-Chou Wu,^{b,d,e,f} Chien-Fu Hung,^{b,f,*} Samuel Achilefu,^{a,g,h} and Kong-Thon Tsen^{i,*}

^aWashington University School of Medicine, Department of Radiology, St. Louis, Missouri 63110, United States

^bJohns Hopkins Medical Institutions, Department of Pathology, Baltimore, Maryland 21231, United States

^cNational Taiwan University, College of Medicine, Taipei 10617, Taiwan

^dJohns Hopkins Medical Institutions, Department of Obstetrics and Gynecology, Baltimore, Maryland 21231, United States

^eJohns Hopkins Medical Institutions, Department of Molecular Microbiology and Immunology, Baltimore, Maryland 21231, United States

^fJohns Hopkins Medical Institutions, Department of Oncology, Baltimore, Maryland 21231, United States

^gWashington University School of Medicine, Department of Biochemistry and Molecular Biophysics, St. Louis, Missouri 63110, United States

^hWashington University School of Medicine, Department of Biomedical Engineering, St. Louis, Missouri 63110, United States

ⁱArizona State University, Department of Physics and Center for Biophysics, Tempe, Arizona 85287, United States

Abstract. There is an urgent need for rapid methods to develop vaccines in response to emerging viral pathogens. Whole inactivated virus (WIV) vaccines represent an ideal strategy for this purpose; however, a universal method for producing safe and immunogenic inactivated vaccines is lacking. Conventional pathogen inactivation methods such as formalin, heat, ultraviolet light, and gamma rays cause structural alterations in vaccines that lead to reduced neutralizing antibody specificity, and in some cases, disastrous T helper type 2-mediated immune pathology. We have evaluated the potential of a visible ultrashort pulsed (USP) laser method to generate safe and immunogenic WIV vaccines without adjuvants. Specifically, we demonstrate that vaccination of mice with laser-inactivated H1N1 influenza virus at about a 10-fold lower dose than that required using conventional formalin-inactivated influenza vaccines results in protection against lethal H1N1 challenge in mice. The virus, inactivated by the USP laser irradiation, has been shown to retain its surface protein structure through hemagglutination assay. Unlike conventional inactivation methods, laser treatment did not generate carbonyl groups in protein, thereby reducing the risk of adverse vaccine-elicited T helper type 2 responses. Therefore, USP laser treatment is an attractive potential strategy to generate WIV vaccines with greater potency and safety than vaccines produced by current inactivation techniques. © The Authors. Published by SPIE under a Creative Commons Attribution 3.0 Unported License. Distribution or reproduction of this work in whole or in part requires full attribution of the original publication, including its DOI. [DOI: [10.1117/1.JBO.20.5.051008](https://doi.org/10.1117/1.JBO.20.5.051008)]

Keywords: ultrashort pulsed lasers; whole inactivated virus vaccines; pathogen inactivation; influenza virus.

Paper 140418SSR received Jun. 30, 2014; accepted for publication Oct. 24, 2014; published online Nov. 25, 2014.

1 Introduction

Emerging viral pathogens are a constant and prominent threat to human health worldwide, as evidenced by the recent outbreak of severe acute respiratory syndrome (SARS), Middle East respiratory syndrome (MERS) coronaviruses, and novel influenza strains with pandemic potential. In addition, there is a persistent risk of engineered viruses derived from bioterrorism. The most logical and cost-effective strategy to protect the human population from these emerging viral diseases is through immunization. Thus, there is a dire need for rapid methods to develop vaccines in response to new viral pathogens.

Whole inactivated virus (WIV) vaccines represent an ideal strategy for this purpose. In contrast to subunit or recombinant vector vaccines, WIV vaccines circumvent the need to identify relevant antigens and can be quickly produced from purified virus using chemical or physical inactivation methods. WIV vaccines contain many of the immunogenic epitopes and immunostimulatory components (such as toll-like receptor ligands) that are needed for an effective virus-specific immune response.

Unfortunately, a general method for producing safe and immunogenic WIV vaccines is lacking. Formalin, an alkylating agent, is one of the most extensively used methods for virus inactivation in the manufacture of vaccines.^{1,2} However, formalin treatment has several crucial limitations: (1) it causes structural damage to B-cell epitopes, which reduces the specificity of antibody responses elicited by the vaccine;³ (2) it generates carbonyl groups in proteins,⁴ a form of oxidative damage that induces harmful and undesirable T helper type 2 (Th2) -biased immune responses;⁵ and (3) it adds unnecessary cost and public concern by introducing a carcinogen into the vaccine. These limitations can be seen in the failure of formalin-inactivated respiratory syncytial virus and measles vaccines, which caused disastrous worsening of the disease upon natural infection.⁶⁻⁹ Alternative methods for virus inactivation, including other alkylating agents, heat, ultraviolet (UV) light, and gamma radiation, all suffer from various combinations of the abovementioned limitations.¹⁰⁻¹³

Recently, a novel method for pathogen inactivation using visible ultrashort pulsed (USP) lasers has been reported (Ref. 14). Visible USP laser treatment inactivates viruses through a physical mechanism: the impulsive stimulated Raman scattering (ISRS) process.^{15,16} There are several theoretical reasons why USP lasers would be advantageous over other methods for

*Address all correspondence to: Kong-Thon Tsen, E-mail: tsen@asu.edu; Chien-Fu Hung, E-mail: chung2@jhmi.edu

WIV vaccine production. Visible light (in the wavelength range of 400 to 700 nm) lacks the photon energy to disrupt covalent bonds in biological macromolecules such as viruses; therefore, USP laser irradiation should not generate Th2 response-inducing carbonyl groups in proteins. In the absence of chromophores, visible light shows negligible intrinsic absorption by proteins and nucleic acids; thus, USP laser irradiation should not denature structural B-cell epitopes through heating. In addition, USP laser irradiation does not induce protein–nucleic acid crosslinking; hence, the TLR-stimulating capacity of viral nucleic acids should be preserved. Furthermore, the USP laser method does not involve introducing any potentially toxic or carcinogenic chemicals during treatment and would alleviate public concerns in those regard. These rationales make the USP laser treatment an attractive potential method to generate safe and effective WIV vaccines.

In this paper, we demonstrate that immunization of mice with the USP laser-inactivated whole inactivated H1N1 influenza virus at about a 10-fold lower dose than that required by conventionally formalin-inactivated H1N1 vaccine results in protection against lethal-dose H1N1 influenza challenge. Splenocytes extracted from mice vaccinated with the USP laser-inactivated virus showed an enhanced influenza-specific cytotoxic T-cell (CTL) response compared with those from unvaccinated mice. In addition, we employed a neutralization assay to confirm the presence of neutralizing antibodies. We demonstrate through hemagglutination assay that the USP laser irradiation has no effect on the surface protein structure of the virus. Furthermore, we have evaluated the effects of USP laser-treatment on a model protein—bovine serum albumin (BSA). We have found that, in contrast to conventional pathogen inactivation methods, the USP laser treatment did not generate Th2 response-inducing carbonyl groups in BSA protein. Therefore, USP laser treatment is a novel and an attractive potential strategy to generate WIV vaccines with greater potency and safety than vaccines produced by current inactivation techniques.

2 Materials and Methods

2.1 Mice

Female BALB/c mice (8 weeks old) were obtained from the National Cancer Institute (Bethesda, Maryland). The mice were kept in a pathogen-free environment at Johns Hopkins University (Baltimore, Maryland).

2.2 Cells

Madin-Darby canine Kidney (MDCK) cells, obtained from ATCC (Manassas, Virginia), were used for all *in vitro* assays. Cells were grown in Dulbecco's modified Eagle's medium (DMEM) with L-glutamine and 10% FBS at 37°C with 5% CO₂.

2.3 Virus

The strain of virus used in this study was A/PR/8/34 (H1N1) from ATCC (Manassas, Virginia). The virus was first grown in MDCK host cells. After centrifugation at 1900 × *g* for 10 min at 4°C, the cell debris was removed. The remaining virus particles were then concentrated by centrifugation at 118,000 × *g* for 1 h at 4°C through a 20% sucrose cushion in phosphate buffered saline (PBS). The virus was stored in aliquots at –80°C. The titer of the virus was measured by the tissue culture infectious dose-50 (TCID₅₀) assay.¹⁷ For the TCID₅₀ assay, MDCK

cells were plated on a 96-well plate. The virus was added in 10-fold dilutions using infection media (DMEM with 4 μg/mL N-acetylated trypsin and 0.03% BSA) for each successive row of wells. The plates were stored in an incubator at 37°C and 5% CO₂. After 4 days, formaldehyde was added to fix the cells and naphthol blue–black was added to stain the fixed cells. The plates were washed and then the 50% infectious dose was calculated using the Reed–Muench method.¹⁸

2.4 Laser Irradiation

The excitation laser source employed in this work was a diode-pumped mode-locked Ti-sapphire laser. The laser produced a continuous train of 65 fs pulses at a repetition rate of 80 MHz.^{14,15,19} The output of the second-harmonic generation of the Ti-sapphire laser was used to irradiate the sample. The excitation laser was chosen to operate at a wavelength of 415 nm and with an average power of 140 mW. It had a pulse width of full width at half maximum of about 100 fs. An achromatic lens of focus length 7.5 cm was used to focus the laser beam into the sample area. In order to facilitate the interaction of the laser with the influenza virus particles, which were placed inside a Pyrex cuvette with buffer solution, a magnetic stirrer was set up so that virions would enter the laser-focused volume. All the laser-irradiated influenza samples contained approximately 2 × 10⁸ TCID₅₀/ml virus and had a volume of about 200 μl. The typical exposure time of the sample to laser irradiation was about 8 h. The diameter of the laser beam was approximately 100 μm within the cuvette and the effective laser exposure time for individual virions was estimated to be about 28 s. The sterility of influenza virus samples after laser treatment was confirmed by TCID₅₀ assay. All the experimental results reported here were obtained at 23°C and with a single laser beam excitation. The temperature increase of sample solutions during USP laser treatments, as monitored by a thermocouple, did not exceed 2°C. The inactivated virus was stored in aliquots at –80°C for use in subsequent vaccination experiments.

2.5 Hemagglutination Assay

Live and the USP laser-inactivated virus preparations were serially twofold-diluted in a 100 ml volume on a 96-well microtitre plate. A 0.5% chicken erythrocyte suspension was added to all wells and plates were incubated for 30 min on ice. This hemagglutination assay was adapted from current protocols in microbiology.²⁰

2.6 Immunization and Challenge

Groups of mice were vaccinated twice at a 2-week interval, as previously described,^{21,22} with 2 × 10⁸/mL TCID₅₀ (20 μl) of laser-inactivated H1N1 virus by intranasal administration. Control mice did not receive vaccine. The mice in both groups maintained a consistent weight prior to administration of the challenge dose. Two weeks after the last vaccination, the mice were challenged with a lethal dose (6 × 10² TCID₅₀) of H1N1, and the weight of the mice was daily monitored. Mice losing more than 25% of their body weight were considered to have reached the experimental endpoint and were euthanized.

2.7 Flow Cytometry

Two weeks after the last vaccination, mice were sacrificed and their splenocytes were isolated and stimulated using influenza

nucleoprotein peptide (NP). Detection of cellular surface CD8a and intracellular IFN- γ was performed using flow cytometry as previously described.²³ Briefly, the cells were incubated for overnight with 1 $\mu\text{g}/\text{ml}$ of GolgiPlug (BD Pharmingen) in the presence of 2 $\mu\text{g}/\text{ml}$ of NP peptide. After washing with FACScan buffer, the cells were stained with phycoerythrin-conjugated anti-mouse CD8a antibody. The cells were then incubated with BD cytofix/cytoperm solution (BD Pharmingen) followed by staining with FITC-conjugated anti-mouse IFN- γ antibody. The splenocytes of all the mice in each group were pooled together and then analyzed by flow cytometry on a Becton-Dickinson FACSCalibur with CellQuest software (BD Biosciences, Mountain View, California). Gating was performed on the lymphocyte area.

2.8 Microneutralization Assay

Blood was collected from the tail vein of vaccinated ($n = 5$) or unvaccinated ($n = 4$) mice 2 weeks after the last vaccination. The serum was stored in aliquots at 4°C. After the serum was collected, the mice were tested for H1N1-specific neutralizing antibodies as follows. 2×10^4 MDCK cells were plated in each well of a 96-well plate. Serum was diluted with infection media (DMEM with 4 $\mu\text{g}/\text{mL}$ N-acetylated trypsin and 0.03% BSA) to 1:100 and added to the first row of wells containing the MDCK cells. After thorough mixing of the well contents, 25 μl of the first row's wells were added to 25 μl of infection media in the next row. This procedure was continued until the last row of wells, resulting in two-fold dilutions, then the extra serum was discarded. A constant H1N1 concentration of 1.75×10^5 TCID₅₀/well was used for each plate. The virus and serum were incubated at 25°C for 2 hours and then added to the 96-well plate with MDCK cells. The plates were stored for three nights in an incubator at 37°C and 5% CO₂. Formaldehyde and naphthol blue-black was added to visualize the results of the reaction as in the TCID₅₀ assay. This assay was repeated three times. Neutralization titers were calculated using the Reed-Muench method. The inverse of the highest dilution at which 50% protection was achieved was determined to be the neutralization titer of the serum.²⁴

2.9 ELISA

The levels of anti-influenza antibodies in sera were determined by a direct enzyme-linked immunosorbent assay (ELISA) as previously described.^{25,26} Briefly, wells of a 96-microwell plate were coated with 100 μl of a 4 $\mu\text{g}/\text{ml}$ of influenza and incubated at 4°C overnight. The wells were then blocked with PBS containing 20% fetal bovine serum. Sera were prepared from the mice on day 14 postimmunization, 100 times diluted in PBS, added to the ELISA wells, and incubated at 37°C for 2 h. After being washed with PBS containing 0.05% Tween 20, the plate was incubated with a 1/2,000 dilution of a peroxidase-conjugated rabbit anti-mouse immunoglobulin G antibody (Zymed, San Francisco, California) at room temperature for 1 h. The plate was washed six times, and then 1-Step Turbo TMB-ELISA was used as a substrate for color development (Pierce, Rockford, Illinois); color development was stopped with 1 M H₂SO₄. The absorbance of the ELISA plate wells was then determined with a standard ELISA reader at 450 nm.

2.10 Protein Carbonyl Quantification

The carbonyl concentrations in untreated BSA, USP laser-treated BSA, or UV-treated BSA were assessed using a dinitrophenylhydrazine (DNPH)-based protein carbonyl colorimetric assay kit (Cayman Chemical) according to the manufacturer's instructions. In the UV treatment group, BSA samples were exposed to a Phillips TUV30W 30-Watt germicidal UVC lamp at a 4-cm distance from the bulb for 90 min.

2.11 Statistical Analysis

Data were analyzed using Microsoft Excel 2010. Each experiment was repeated in duplicate or triplicate. Individual data points were compared using Student's *t* test.

3 Experimental Results

3.1 Effect of the Ultrashort Pulsed Laser Virus Inactivation on Hemagglutination Activity

Hemagglutination activity after the USP laser virus inactivation provides one indicator to the structural alternation of the surface proteins of the virus inactivation treatment. Purified influenza stock was aliquoted into batches and treated with the USP laser irradiation. Following the complete loss of infectivity, we compared the hemagglutination activity of live and inactivated viruses. As shown in Table 1, within the experimental uncertainty, hemagglutination activity was not affected by the USP laser irradiation. These results provide evidence that the USP laser irradiation, among other inactivation methods, causes the least structural changes to viral surface proteins.

3.2 Laser-Inactivated H1N1 Influenza Vaccine Confers Protection against Lethal H1N1 Challenge in Mice

We determined whether the laser-inactivated H1N1 virus vaccine conferred protection against a lethal dose of H1N1. The percent of change from initial weight was used as an indicator of the health of the mice. Groups of mice received vaccination ($n = 8$) or no treatment ($n = 8$). Two weeks after the last vaccination, mice in both groups were given a lethal dose of 6×10^2 TCID₅₀/mL live H1N1 virus. Following administration of the challenge dose, the weights of mice in the control group rapidly decreased. As shown in Fig. 1, by the seventh day after receiving the challenge dose, control mice lost a significant percentage of their initial weight, while the mice in the vaccinated group maintained healthy weights. Our results show that vaccination is 87.5% effective against a challenge of lethal dose.

Table 1 Hemagglutination activity of live and the ultrashort pulsed (USP) laser-inactivated influenza virus with A/PR/8/34 strain.

Strain	Method of inactivation	HAU/ml
A/PR/8/34	Original live stock	$(2.3 \pm 0.2) \times 10^5$
	USP laser inactivation	$(2.1 \pm 0.2) \times 10^5$

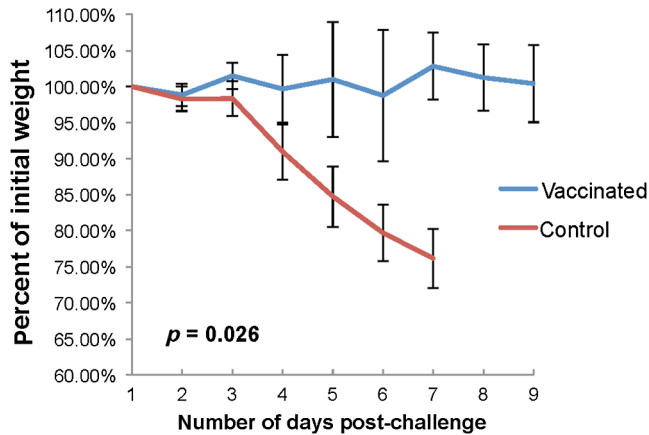


Fig. 1 Body weight changes in H1N1-challenged mice. Groups of BALB/c mice ($n = 8$) were vaccinated twice with 2×10^8 TCID₅₀/ml ($20 \mu\text{l}$) of laser-inactivated H1N1 virus by intranasal administration at a 2-week interval, or received no treatment. 21 days later, all mice were challenged with a lethal dose of 6×10^2 TCID₅₀/mL of A/PR/8/34 influenza virus. Following lethal challenge, mice were monitored for percent change of initial weight for 9 days. Each point represents the mean and bars represent standard deviation. (Student's t test comparing the final weights of each group of mice, $P = 0.026$).

3.3 Laser-Inactivated H1N1 Influenza Vaccine Increases CD8⁺ Immune Response in Mice

To further investigate the immunity generated by vaccination with laser-inactivated virus, CTL activation was assessed. Splenocytes were obtained from vaccinated or untreated mice and stimulated by immunogenic influenza NP peptide. Cells were fluorescently tagged for CD8 and IFN- γ and analyzed by flow cytometry. Figure 2 demonstrates that the vaccinated mice show a 10-fold increase in the percentage of activated NP peptide-specific T cells in comparison to the control mice. These data indicate that vaccination with laser-inactivated virus

generates influenza antigen-specific CD8⁺ T cell immune responses.

3.4 Laser-Inactivated H1N1 Influenza Vaccine Generates Influenza-Specific Neutralizing Antibodies

We next investigated humoral immunity induced by vaccination using a microneutralization assay. This neutralization assay is a sensitive and specific technique to measure neutralizing antibody responses to H1N1 virus. As shown in Fig. 3, we found that sera from mice that received laser-inactivated vaccination showed a significantly higher neutralizing antibody titer compared to sera from control (unvaccinated) mice. Furthermore, we observed that vaccination with decreasing doses of laser-inactivated influenza virus generated virus-specific antibody responses to lesser degrees. These experimental results indicate that vaccination with laser-inactivated virus induces neutralizing antibody immune responses.

3.5 Transmission Electron Microscopy Images Reveal that the Laser-Inactivated Virus Retains Its Global Viral Structure

We used transmission electron microscopy (TEM) to visually examine the active and laser-inactivated influenza viruses. Figures 4(a) and 4(b) show the TEM images of the influenza virus with or without laser irradiation, respectively. We have found that the global structure of the virus is maintained after the USP laser treatment, indicative of the production of WIV by the USP laser irradiation.

3.6 Laser Treatment Does Not Generate Carbonyl Groups in Protein

Conventional inactivation methods including formalin, UV treatment, and gamma radiation are potent inducers of carbonyl

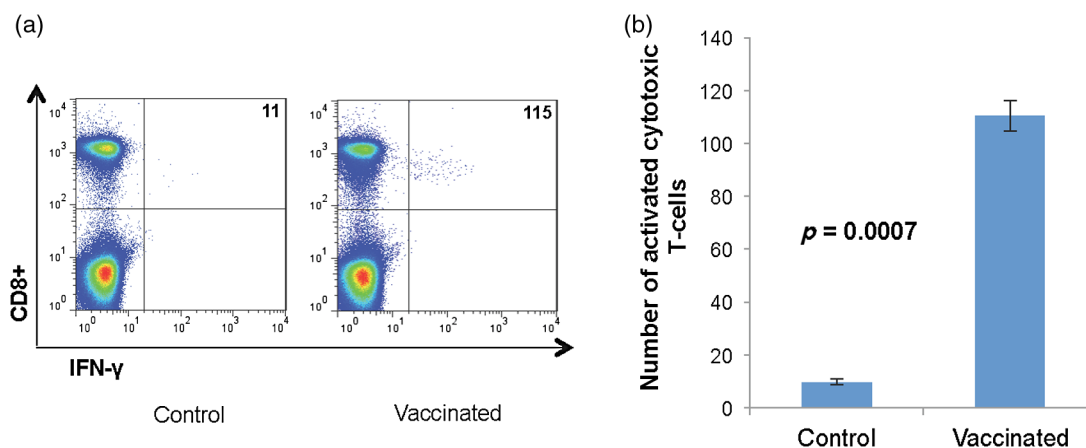


Fig. 2 CD8⁺ T cell induction following vaccination. Splenocytes were isolated from vaccinated and untreated BALB/c mice and then the cells were incubated overnight in the presence of $2 \mu\text{g}/\text{ml}$ of NP peptide. After washing with FACScan buffer, the cells were stained with phycoerythrin-conjugated anti-mouse CD8a antibody, followed by fixing/permeabilizing and staining with FITC-conjugated anti-mouse IFN- γ antibody. The splenocytes were then analyzed by flow cytometry on a FACSCalibur with CellQuest software, and gated on the lymphocyte area. (a) Representative flow cytometry analysis. The upper right-hand quadrant shows the percentage of NP-specific, IFN- γ secreting CD8⁺ T cells among lymphocytes. (b) Bar graph depicting the percentage of activated CD8⁺ T cells among splenocytes in vaccinated and unvaccinated mice ($P < 0.001$).

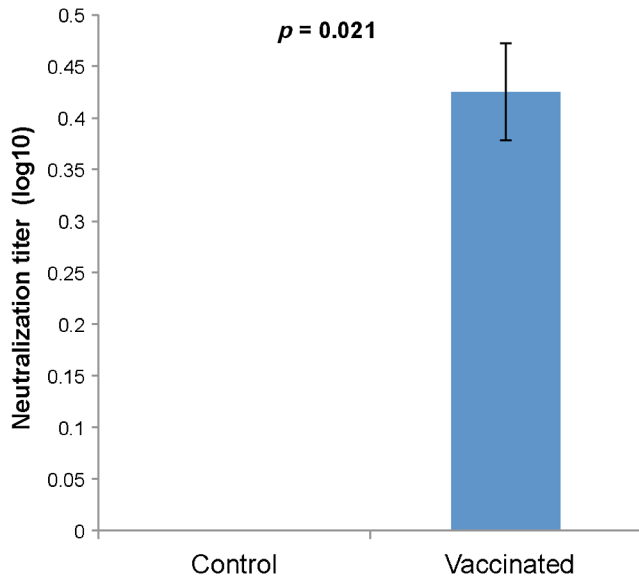


Fig. 3 Neutralizing antibodies detected by microneutralization assay. Serum from vaccinated ($n = 5$) and unvaccinated ($n = 4$) groups of mice was extracted 20 days after vaccination and then added to Madin-Darby canine kidney (MDCK) cells in a 96-well plate, serially diluted, and incubated for 3 days. Subsequently, a constant H1N1 concentration of 1.75×10^5 TCID₅₀/well was used for each plate. The virus and serum were incubated at 25°C for 2 h and then added to the 96-well plate with MDCK cells. The plates were stored for three nights in an incubator at 37°C and 5% CO₂. Formaldehyde and naphthol blue-black was added to visualize the results of the reaction. The presence of neutralizing antibodies was determined by cell survival. Neutralization titers were calculated using the Reed–Muench method. Bar graph depicts neutralization titer of untreated and vaccinated mice. ($P = 0.021$).

groups in protein;^{4,10,11,27} these carbonyl groups are in turn inducers of harmful and undesirable T helper type 2 responses.^{4,5} To determine whether laser treatment generates protein carbonylation, we used a colorimetric 2,4-dinitrophenylhydrazine (DNPH)-based assay to quantitate carbonyl content in laser-treated BSA. Untreated BSA or UV-treated BSA served as negative and positive controls, respectively. Figure 5 shows that there is no significant increase in carbonyl content in laser-treated BSA samples relative to untreated BSA. In contrast, the carbonyl content of the UV-treated BSA was dramatically increased relative to both untreated and laser-treated BSAs ($p = 0.0004$). These results demonstrate that USP laser treatment generates fewer carbonyl groups in protein antigens compared with conventional pathogen inactivation methods, reducing the risk of detrimental vaccine-elicited Th2 responses.

4 Discussion

Because of the following two reasons, the complete inactivation of H1N1 flu viruses in the sample by the USP laser irradiation observed in our experiments and used for the vaccine cannot be due to the two-photon absorption effect. First, we have estimated the number of UVC photons which might be produced at the laser power densities used in our experiments. The two-photon absorption coefficient for H1N1 flu virus is not available in the literature; however, if we assume that the viruses are giant molecules and that their two-photon absorption coefficient at 415 nm is comparable to that of a typical molecule,²⁸ then the number of UVC photons at 208 nm generated under our experimental conditions was estimated to be of the order of

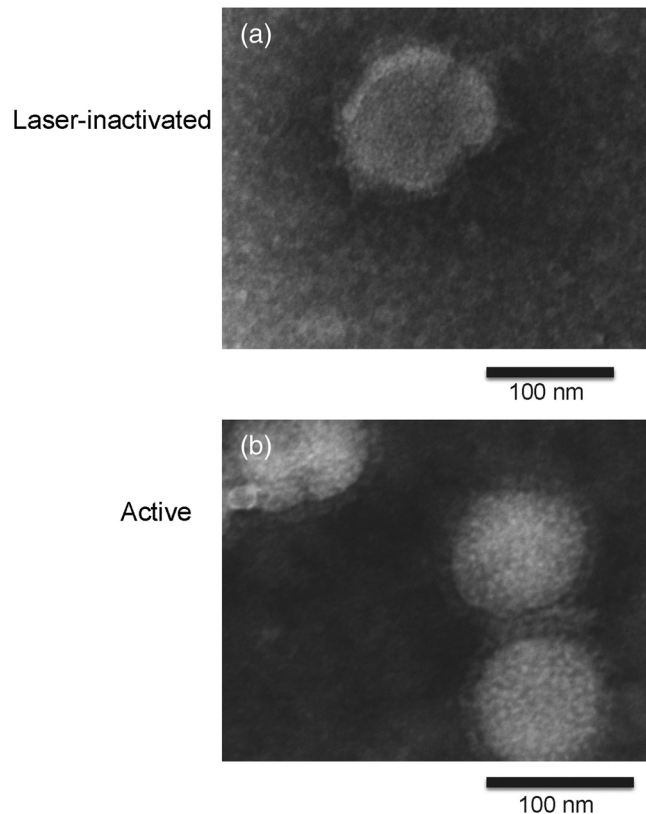


Fig. 4 Transmission electron microscopy (TEM) images of influenza virus. Samples of laser-inactivated and active A/PR/8/34 influenza virus were fixed with glutaraldehyde and visualized using TEM. (a) Fixed sample of laser-inactivated virus at 93,000× magnification. (b) Fixed sample of the active virus at 93,000× magnification. These TEM images demonstrate the retention of capsid and global structure of the influenza virus after the ultrashort pulsed (USP) laser irradiation and provide support for the laser-induced protein aggregation through ISRS process for the most likely inactivation mechanism.

0.1/ second. Because the laser exposure time is 8 h, the number of generated UVC photons is about 3000 for the total laser exposure time. On the other hand, the total number of H1N1 viral particles in the laser-irradiated sample is about 200 million; since one UVC photon at 208 nm can inactivate only one viral particle, the value of generated UVC photons of about 3000 during the total laser exposure time is too small to account for the complete inactivation of 200 million viral particles observed in our experiments. Second, we have tried to detect the UVC photons which might be generated in our laser experiments (here, the glass vial is replaced by a synthetic fused silica vial) by using a UV spectrometer with a photon counting system. Within our experimental uncertainty of ± 0.5 photon/second, we failed to detect any of the UVC photons at 208 nm. This finding is consistent with our estimation stated above. In addition, we note that the absorption coefficient of water at 208 nm is about 0.05 cm^{-1} , which means that the effect of water absorption at 208 nm is negligible and cannot be the reason for not detecting the UVC photon. Therefore, the observed complete inactivation for H1N1 flu virus observed in our experiments cannot be due to UVC photons generated by two-photon absorption.

It has been shown that nonenveloped viruses such as murine norovirus (MNV) are inactivated by a visible USP laser through the ISRS process,¹⁶ whereby the USP laser pulses excite Raman-active vibrational modes on the capsid of the nonenveloped

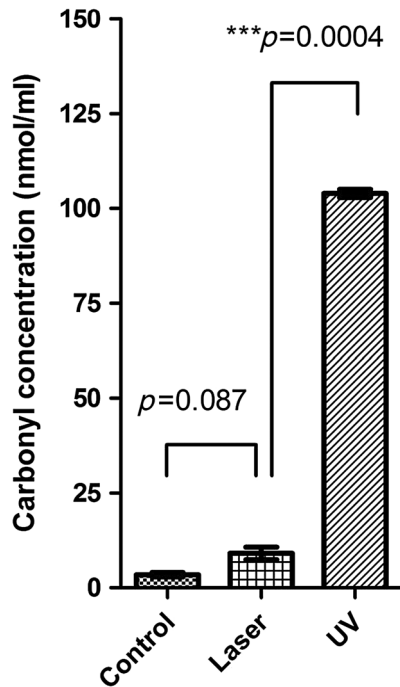


Fig. 5 Carbonyl content of laser-treated bovine serum albumin (BSA) protein. The carbonyl concentrations in untreated BSA, USP laser-treated BSA, or UV-treated BSA were assessed using a dinitrophenylhydrazine (DNPH) protein carbonyl colorimetric assay kit. Untreated BSA served as negative control; UV-treated BSA served as positive control.

virus—MNV. The amplitude of the vibration is linearly proportional to the laser intensity. When the laser intensity is sufficiently large, the excited amplitude of vibration on the capsid can become extremely large, leading to the breaking of weak links such as hydrogen bonds and hydrophobic contacts in the capsid of the virus. This causes the capsid to disintegrate into subunits. The virus becomes inactivated because of the loss of integrity of its capsid. On the other hand, it has been demonstrated that enveloped viruses such as murine cytomegalovirus (MCMV) are inactivated by a visible USP laser via the ISRS process as well but through a different route/pathway.¹⁹ The USP laser pulses excite Raman-active modes on the proteins of the capsid as well as the tegument proteins of the enveloped virus—MCMV through the impulsive stimulated Raman scattering process. The excitations, which break the hydrogen bonds and hydrophobic contacts on these proteins, cause partial unfolding of the proteins. These unfolded proteins will rapidly reform their broken weak hydrogen bonds and hydrophobic contacts and return to their original folded configuration. However, if the concentration of proteins is very high, such as in the case of proteins confined within the capsid of a virus, they can form hydrogen bonds and hydrophobic contacts with other proteins nearby, leading to the aggregation of proteins. This has been the case for the enveloped virus—MCMV. Aggregation between capsid proteins and tegument proteins has been found to be the cause of inactivation for an enveloped virus. All influenza viruses are enveloped viruses. Therefore, we believe that the most likely inactivation mechanism for the H1N1 influenza virus inactivated by the visible USP laser studied here is the ISRS process. The TEM images of H1N1 influenza virus before and after the USP laser irradiation, shown in Fig. 4, further support our argument. The striking

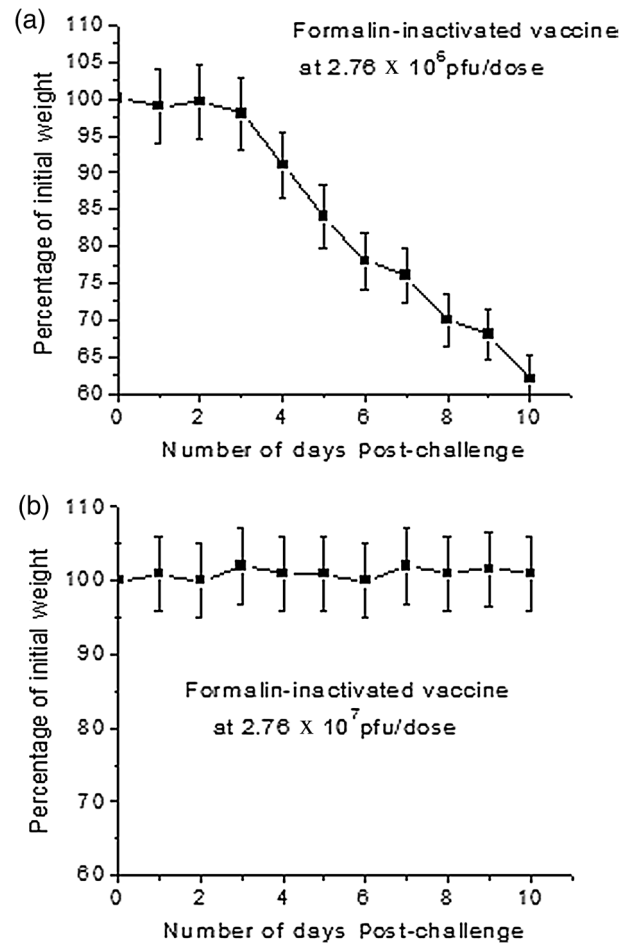


Fig. 6 Body weight changes in H1N1-challenged mice vaccinated with conventional formalin-inactivated vaccine. (a) One control group vaccinated with two doses of conventional formalin-inactivated H1N1 vaccine at $\approx 2.76 \times 10^6$ pfu/dose; (b) the other control group vaccinated with two doses of conventional formalin-inactivated H1N1 vaccine at $\approx 2.76 \times 10^7$ pfu/dose. The mice of the control group in (a) all died (the weights decreased more than 30% of their initial ones) 10 days after challenging; whereas the mice of the control group in (b) achieved 75% protection.

similarity between these TEM images to those of MCMV,¹⁹ i.e., the retention of the capsid and the global structure of the virus, suggests that the effects (and, therefore, the underlying inactivation mechanism) of the USP laser irradiation on these two enveloped viruses are the same.

To give a perspective on the vaccine potency reported in our current study, it is illustrative to compare the vaccine dosages required for protection against lethal challenge in mice using conventional or laser-inactivated H1N1 influenza vaccines. Among conventional methods including heat, formalin, beta propiolactone, and detergents, formalin was found to have the greatest preservation of influenza vaccine antigens.¹³ We have performed additional experiments in which two control groups of mice got conventional formalin-inactivated H1N1 influenza vaccine. Figure 6(a) shows one control group vaccinated with two doses of conventional formalin-inactivated H1N1 vaccine at $\approx 2.76 \times 10^6$ pfu/dose, which was the dose of the USP laser-inactivated vaccine that we used for protection against the challenge. Figure 6(b) shows the other control group vaccinated with two doses of conventional formalin-inactivated H1N1 vaccine at

$\approx 2.76 \times 10^7$ pfu/dose. The mice of the control group in Fig. 6(a) all died (the weights decreased more than 30% of their initial ones) 10 days after challenging; whereas the mice of the control group in Fig. 6(b) achieved 75% protection. On the other hand, with the visible USP laser irradiation method, we employed two doses of USP laser-inactivated vaccine at $\approx 2.76 \times 10^6$ pfu/dose, which is a 10-fold lower dose relative to the formalin-inactivated vaccine, to achieve 87.5% protection. Therefore, these results indicate that the USP laser-inactivated vaccine is significantly more efficient than the vaccine prepared by the conventional formalin-inactivated vaccine.

The relatively high potency of the USP laser-inactivated influenza virus vaccine can be partly attributed to the fact that the visible USP laser irradiation has minimal effects on the structure of proteins. The circular dichroism (CD) spectrum of BSA protein measured before and after the USP laser irradiation is a good example. The CD spectrum is very sensitive to the secondary structure of proteins. It has been shown that, within experimental uncertainty, there is no change in the CD spectrum of BSA protein before and after USP laser irradiation.¹⁵ These spectroscopic results are in line with our hemagglutination activity results. Our experimental results on the hemagglutination activity of the virus show that, within the experimental uncertainty, the USP laser irradiation has no effects on the surface protein structure of the virus.

We note that the USP laser-inactivated influenza vaccine may generate heterosubtypic immunity, which is the aim of current efforts to design universal influenza vaccines. The CTL response is a key mechanism for improved heterosubtypic protection against influenza because CTLs have been shown to be specific for epitopes that are conserved among viral subtypes.²⁹ Our data showed that splenocytes from vaccinated mice showed a 10-fold increase of influenza NP-specific CTLs compared to unvaccinated mice. These results suggest that the laser-inactivated influenza vaccine has the potential to generate cross-protection against multiple strains and address the issue of viral mutation.

The presence of carbonyl groups in vaccine antigens has been linked to the induction of undesirable and potentially deleterious Th2-mediated immunopathology.^{4,5} Many inactivation techniques including UV and gamma radiation are potent inducers of protein carbonylation.^{4,10,11,27} We note that although formaldehyde is not an oxidizing agent and cannot produce oxidative damage in a cell free system, the carbonyl groups introduced into proteins by formaldehyde in the formalin inactivation technique have something in common with the carbonyl groups introduced by protein oxidation.

In contrast to these techniques, visible USP lasers lack the energy to disrupt covalent structures in proteins. Therefore, we reasoned that USP laser treatment would not cause protein carbonylation. The experimental results in Fig. 5 confirm this. These data demonstrate that USP laser treatment does not generate significant levels of carbonyl groups in protein antigens compared with conventional pathogen inactivation methods, reducing the risk of detrimental vaccine-elicited Th2 responses. In addition to carbonyl groups, other types of covalent damage caused by formalin, UV, and gamma radiation can result in the formation of "neoantigens" and elicit adverse immune reactions when administered to patients, as was seen in penicillin allergies³⁰ and certain chemically treated blood products.³¹ In contrast, the USP laser inactivates enveloped influenza virus through the disruption of weak, noncovalent hydrogen bonds

and hydrophobic contacts in the virion, leading to the aggregation of capsid and tegument proteins. As a result, there is an overall reduced concern of side effects from vaccines prepared by the USP laser treatment method.

5 Conclusion

In summary, we have demonstrated a novel USP laser irradiation method for the production of safe and potent WIV vaccines. We envision that the future of pathogen inactivation technologies will favor chemical-free methods that target properties specific to pathogens while preserving desirable components of the treated product, leading to improved safety profiles. The USP laser irradiation method we have presented in this report is one such potential technology. Further, evaluation of the USP laser-inactivated vaccine for cross-protection and in the context of other important pathogens such as HIV, SARS, and MERS is warranted.

Acknowledgments

This work was supported in part by NHLBI Ruth L. Kirschstein NRSA F30 under Grant No. HL116183-01 (SDT), the Mallinckrodt Institute of Radiology Development Fund, and NIH under Grant Nos. R01 EB008111 and R33 CA123537 (SA).

References

1. E. S. Mocarski, T. Shenk, and R. F. Pass, *Fields Virology*, pp. 2701–2772, Lippincott Williams and Wilkins, Philadelphia, Pennsylvania (2007).
2. N. Bardiyah and J. H. Bae, "Influenza vaccines: recent advances in production technologies," *Appl. Microbiol. Biotechnol.* **67**, 299–305 (2005).
3. N. K. Blackburn and T. G. Besselaar, "A study of the effect of chemical inactivants on the epitopes of Rift Valley fever virus glycoproteins using monoclonal antibodies," *J. Virol. Methods* **33**, 367–374 (1991).
4. A. Moghaddam et al., "A potential molecular mechanism for hypersensitivity caused by formalin-inactivated vaccines," *Nat. Med.* **12**, 905–907 (2006).
5. A. E. Moghaddam et al., "Reactive carbonyls are a major Th2-inducing damage-associated molecular pattern generated by oxidative stress," *J. Immunol.* **187**, 1626–1633 (2011).
6. J. Chin et al., "Field evaluation of a respiratory syncytial virus vaccine and a trivalent parainfluenza virus vaccine in a pediatric population," *Am. J. Epidemiol.* **89**, 449–463 (1969).
7. V. A. Fulginiti et al., "Respiratory virus immunization. I. A field trial of two inactivated respiratory virus vaccines; an aqueous trivalent parainfluenza virus vaccine and an alum-precipitated respiratory syncytial virus vaccine," *Am. J. Epidemiol.* **89**, 435–448 (1969).
8. H. W. Kim et al., "Respiratory syncytial virus disease in infants despite prior administration of antigenic inactivated vaccine," *Am. J. Epidemiol.* **89**, 422–434 (1969).
9. A. Z. Kapikian et al., "An epidemiologic study of altered clinical reactivity to respiratory syncytial (RS) virus infection in children previously vaccinated with an inactivated RS virus vaccine," *Am. J. Epidemiol.* **89**, 405–421 (1969).
10. C. S. Sander et al., "Photoaging is associated with protein oxidation in human skin in vivo," *J. Invest. Dermatol.* **118**, 618–625 (2002).
11. D. Scheidegger et al., "Protein oxidative changes in whole and skim milk after ultraviolet or fluorescent light exposure," *J. Dairy Sci.* **93**, 5101–5109 (2010).
12. S. De Flora and G. Badolati "Thermal inactivation of untreated and gamma-irradiated A2-Aichi-2-68 influenza virus," *J. General Virol.* **20**, 261–265 (1973).
13. M. Jonges et al., "Influenza virus inactivation for studies of antigenicity and phenotypic neuraminidase inhibitor resistance profiling," *J. Clin. Microbiol.* **48**, 928–940 (2010).
14. S. W. Tsen et al., "Prospects for a novel ultrashort pulsed laser technology for pathogen inactivation," *J. Biomed. Sci.* **19**, 62 (2012).

15. K. T. Tsen et al., "Studies of inactivation of encephalomyocarditis virus, M13 bacteriophage, and Salmonella typhimurium by using a visible femtosecond laser: insight into the possible inactivation mechanisms," *J. Biomed. Opt.* **16**, 078003 (2011).
16. S. W. Tsen et al., "Studies of inactivation mechanism of non-enveloped icosahedral virus by a visible ultrashort pulsed laser," *Virol. J.* **11**, 20 (2014).
17. D. D. LaBarre and R. J. Lowy, "Improvements in methods for calculating virus titer estimates from TCID50 and plaque assays," *J. Virol. Methods* **96**, 107–126 (2001).
18. L. J. Reed and H. Muench, "A simple method of estimating fifty per cent endpoints," *Am. J. Hyg.* **27**, 493–497 (1938).
19. S. W. Tsen et al., "Inactivation of enveloped virus by laser-driven protein aggregation," *J. Biomed. Opt.* **17**, 128002 (2012).
20. K. J. Szretter, A. L. Balish, and J. M. Katz, "Influenza: propagation, quantification, and storage," Chapter 15 in *Current Protocols in Microbiology*, Vol. **1**, John Wiley & Sons, Inc, New Jersey (2006).
21. B. Manicassamy et al., "Protection of mice against lethal challenge with 2009 H1N1 influenza A virus by 1918-like and classical swine H1N1 based vaccines," *PLoS Pathog.* **6**, e1000745 (2010).
22. C. Savard et al., "Improvement of the trivalent inactivated flu vaccine using PapMV nanoparticles," *PLoS One* **6**, e21522 (2011).
23. S. Peng et al., "Characterization of HPV-16 E6 DNA vaccines employing intracellular targeting and intercellular spreading strategies," *J. Biomed. Sci.* **12**, 689–700 (2005).
24. R. E. Wooley et al., "Comparison of a microneutralization test in cell culture and virus neutralization test in embryonated eggs for determining infectious bronchitis virus antibodies," *J. Clin. Microbiol.* **3**, 149–156 (1976).
25. F. S. Quan et al., "Kinetics of immune responses to influenza virus-like particles and dose-dependence of protection with a single vaccination," *J. Virol.* **83**, 4489–4497 (2009).
26. F. S. Quan et al., "Virus-like particle vaccine induces protective immunity against homologous and heterologous strains of influenza virus," *J. Virol.* **81**, 3514–3524 (2007).
27. A. Krisko and M. Radman, "Protein damage and death by radiation in Escherichia coli and Deinococcus radiodurans," *Proc. Natl. Acad. Sci. U. S. Am.* **107**, 14373–14377 (2010).
28. R. W. Boyd, *Nonlinear Optics*, Academic Press, San Diego, California (1992).
29. M. Schotsaert, X. Saelens, and G. Leroux-Roels, "Influenza vaccines: t-cell responses deserve more attention," *Expert Rev. Vaccines* **11**, 949–962 (2012).
30. X. Meng et al., "Direct evidence for the formation of diastereoisomeric benzylpenicilloyl haptens from benzylpenicillin and benzylpenicillenic acid in patients," *J. Pharmacol. Exp. Ther.* **338**, 841–849 (2011).
31. P. M. Sobral et al., "Viral inactivation in hemotherapy: systematic review on inactivators with action on nucleic acids," *Revista brasileira de hematologia e hemoterapia* **34**, 231–235 (2012).

Biographies of the authors are not available.